RSC Advances

PAPER

View Article Online
View Journal | View Issue

Cite this: *RSC Adv.*, 2021, **11**, 39958

Facile synthesis of dual-emission fluorescent carbon nanodots for a multifunctional probe†

Chin-Wei Cheng, Kuan-Min Lo, Min-Feng Li, Tai-Chia Chiu and Cho-Chun Hu *

Received 23rd October 2021
Accepted 6th December 2021

DOI: 10.1039/d1ra07826g

rsc.li/rsc-advances

In this study, we developed a facile method for synthesizing dual-emission carbon nanodots (CDs) through trimesic acid and *o*-phenylenediamine through electrolysis for 2 h. The synthesized CDs were mainly 3–7 nm in size, with an average size of 5.17 nm. The dual-emission fluorescent property of these CDs could be observed under two different excitation wavelengths. The green emission of the CDs could be quenched after the addition of mercury ions or copper ions, and the blue emission of the CDs could be inhibited using hydroxychloroquine (HCQ). Furthermore, the quenched fluorescence of CDs/Cu^{2+} could be recovered through the addition of glyphosate. We developed a multifunctional chemical sensor by using these special fluorescence materials. Under optimal conditions, the detection limits of mercury ions, glyphosate, and HCQ were 0.42 μM, 1.1 mg L^{-1}, and 0.14 μM, respectively. Moreover, this method can be used to detect mercury ions, glyphosate, and HCQ in environmental water, cereals, and urine samples, respectively.

1. Introduction

Over the past years, carbon nanodots (CDs) as a new type of material have been widely applied in many fields because of their unique fluorescent and chemical affinity properties. Many CD synthesis strategies, such as microwave radiation,[1] thermal assisted pyrolysis,[2] hydrothermal,[3] electrochemical[4] and ultrasonic assisted synthesis,[5] have been developed. Among these methods, electrochemical synthesis offers simple, low-cost, and low-pressure operation that can be performed at room temperature. Furthermore, this bottom-up electrochemical synthesis method can be used to easily adjust the size and the functional group on the CDs. Thus, the optical and chemical properties of the CDs could be modified and customized conveniently. Electrochemically synthesized CDs can potentially be used in applications such as biomedical imaging,[6] photocatalysis,[7] sensors,[8] and white light-emitting diodes (LEDs).[9] Among these applications, CDs as sensors are the most commonly used for the detection of metal ions,[10] medicines,[11] pesticides,[12] and so on. However, most of these CDs can only be used as single functional sensors because of their original specific fluorescence properties.

The discharge of industrial wastewater containing mercury ions has caused severe environmental pollution. This mercury can make its way into the food chain and be consumed by humans, causing aliments such as muscle weakness, paresthesia, and even Minamata disease.[13] Furthermore, pollution resulting from pesticides also caused several environmental problems.

In recent years, glyphosate has been commonly used in agriculture, horticulture, viticulture and afforestation, and garden maintenance because of its low cost and wide availability. However, glyphosate residues can pollute the environment and enter the food chain because of their long half-life and excellent water solubility.[14] Glyphosate has been classified as probably carcinogenic to humans.[15] Therefore, quantification of Hg^{2+} and glyphosate in the environment matrix is crucial.

Hydroxychloroquine (HCQ) has been used as a medication for treating malaria or lupus erythematosus for approximately 65 years. Furthermore, HCQ has potential for COVID-19.[16] A method for easily detecting HCQ in patients' urine can aid clinical diagnosis and treatment.

In this study, CDs were synthesized electrochemically from trimesic acid and *o*-phenylenediamine. Compared with other synthetic methods, our method is more convenient and environmentally friendly. The prepared CDs were used to detect Hg^{2+}, glyphosate, and HCQ. The results revealed that the fluorescence of these CDs could be quenched by Hg^{2+} (or Cu^{2+}). Furthermore, the addition of glyphosate can restore the fluorescence of the CDs/Cu^{2+} complex because of the high capability coordination between the glyphosate and copper ions. When HCQ was added to a CD aqueous solution, the fluorescence of the CDs was quenched because of the inner filter effect (IFE). Moreover, methods for the quantification of Hg^{2+}, glyphosate, and HCQ in real samples were also successfully developed.

Department of Applied Science, National Taitung University, Taiwan, Republic of China. E-mail: cchu@nttu.edu.tw

† Electronic supplementary information (ESI) available. See DOI: 10.1039/d1ra07826g

2. Experimental sections

2.1 Materials

Trimesic acid (TMA) and *o*-phenylenediamine (*o*PD) were obtained from Alfa Aesar (U.S.A.). Other chemicals were purchased from Sigma-Aldrich (U.S.A.). All reagents were analytical grade and used directly without any further purification. Ultrapure water with a resistivity of 18.2 MΩ cm was used throughout the experiment. Material purification was carried out using 3500 Da cutoff membranes (Amicon Ultra-4, Millipore).

2.2 Apparatus

Fluorescence measurements were performed by using a Shimadzu RF-6000 spectrofluorophotometer (Kyoto, Japan). The ultraviolet-visible (UV-vis) spectra were obtained by a Hitachi U-2900 UV-vis spectrophotometer (Tokyo, Japan). The transmission electron microscope (TEM) images were taken on a PHILIPS CM-200 TWIN TEM (Amsterdam, Netherlands). X-ray photoelectron spectroscopy (XPS) was measured by a Thermo K-Alpha (Thermo Fisher, USA.). Zeta potential measurements were performed on a Zetasizer Nano-ZS90 (Malvern, UK).

2.3 Synthesis of the duel-emissive CDs

The CDs were synthesized by a easy and one-step electrochemical method. Trimesic acid (TMA) and *o*-phenylenediamine (*o*PD) appropriate proportion were added to 0.1 M NaOH (10 mL) to form a transparent solution under stirring. Two platinum rods (6 cm × 0.1 cm) were employed as the positive and negative electrodes, respectively. The distance between the two rods was about 1 cm. The reaction proceeded for 2 h at 10 V potential (DC). After 2 h, the solution would turn from transparent to dark brown. The solution was centrifuged at 10 000 rpm at 15 °C for 10 min to remove large particles. The obtained dark brown solution was filtered through a microporous filtering film (0.22 μm). The colloidal solution was repeatedly dialyzed against ultrapure water in a dialysis bag (3500 Da) for 6 h. The dark brown solution was obtained and stored at 4 °C.

2.4 Detection of Hg^{2+} using the CDs

The detection of Hg^{2+} was performed at room temperature in pH 6.0, 10 mM phosphate buffer solution (PBS). Different concentrations of Hg^{2+} (1 mL each) were separately added into the mixture of 200 μL of the CDs solution and 200 μL of phosphate buffer (pH 6.0). The total volume of the solution was 2 mL. The fluorescence intensity spectra were recorded under excitation at 390 nm. In order to detect the specificity of the CDs to the Hg^{2+}, the other metal ions were added to the CDs under the same condition. All the experiments were performed at room temperature (Scheme 1).

2.5 Detection of glyphosate

At first, 600 μL of glyphosate within a concentration range of 0–100 mg L^{-1} was added to 1 mL Cu^{2+} (0.1 mM) solution. After vigorously shaking, 200 μL of phosphate buffer (0.1 M, pH 6) and 200 μL of the CDs were added successively. The fluorescence intensity spectra were recorded under excitation at 390 nm.

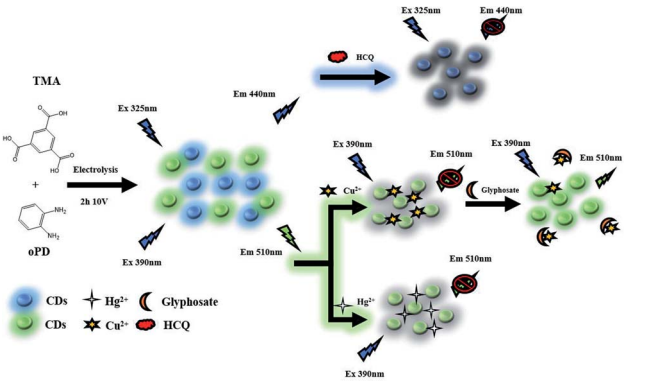

Scheme 1 Schematic illustration for the synthetic procedure of CDs and detection of mercury ion, glyphosate and hydroxychloroquine.

2.6 Detection of hydroxychloroquine

The following procedure was adopted for the detection of hydroxychloroquine: 200 μL of the CDs, 200 μL of 0.1 M phosphate buffer, and 600 μL of distilled deionized water were placed in a 2 mL centrifugal tube. Then, 1 mL of hydroxychloroquine within a concentration range of 0–1000 μM was added into the above solution. The mixture solution was incubated at 25 °C for 30 min as well, and then the fluorescence spectra of the mixture solution were recorded under excitation at 325 nm.

2.7 Real sample detection

2.7.1 Calculation of Hg^{2+} recovery in real samples. The lake water samples were collected from the Jingxin Lake, National Taitung University. The water samples were spiked with standard Hg^{2+} solution. Then all the water samples used in the experiments were centrifuged at 8000 rpm and filtered through 0.22 μm membrane before analysis.

2.7.2 Calculation of glyphosate recovery in real samples. The water samples were spiked with standard glyphosate solution. The purification of all the water samples was the same as the purification of the water samples spiked with standard glyphosate solution. 2 g of the cereals sample was put into the centrifuge tube, and 10 mL ultrapure water was added. Then the mixture stood still for 10 min. After that, the 10 mL methanol containing 1% formic acid was added into the centrifuge tube and shaken by hand for 1 min. After keeping for 1 min, the mixture was centrifuged at 5000 rpm for 10 min. 2 mL supernatant was evaporated and re-dissolved with 2 mL ultrapure water. Then, different concentrations of glyphosate standard solutions were added into cereals samples.

2.7.3 Calculation of hydroxychloroquine recovery in real samples. The artificial urine sample was prepared according to the work.[17] With $CaCl_2$ (0.65 g L^{-1}), $MgCl_2$ (0.65 g L^{-1}), NaCl (4.6 g L^{-1}), Na_2SO_4 (2.3 g L^{-1}), $Na_3C_3H_5O(CO_2)_3$ (0.65 g L^{-1}),

$Na_2C_2O_4$ (0.02 g L^{-1}), KH_2PO_4 (2.8 g L^{-1}), KCl (1.6 g L^{-1}), NH_4Cl (1.0 g L^{-1}), urea (25.0 g L^{-1}), creatinine (1.1 g L^{-1}) and dextrose (0.3%). The urine samples were collected from humans who hadn't taken any medicine in the last three months. The urine samples were subject to a 100-fold dilution before analysis.[10] Diluted samples were spiked with various concentrations of standard HCQ solution.

3. Results and discussion

3.1 The synthesis and characterization of the CDs

CDs synthesis was performed through electrochemical processing for 2 h with a DC voltage of 10 V. To obtain CDs with the most appropriate fluorescence properties, we investigated the effect of the ratio of the two starting materials (TMA and *o*PD). Various CDs were synthesized for various ratios of the TMA and *o*PD from 0 : 9 to 1 : 1. The CDs synthesized at the TMA and *o*PD ratio of 1 : 8 exhibited the strongest fluorescent properties and were selected as probes for further application (Table S1†).

The structure of the CDs was investigated through X-ray photoelectron spectroscopy (XPS). The Fig. 1A shows the full scan XPS spectrum of the CDs. Three peaks at 284.6 eV, 399.6 eV and 531.6 eV corresponded to C 1s, N 1s and O 1s, respectively. The products consisted of C (atomic%: 64.69%), N (atomic%: 12.16%), and O (atomic%:16.37%). The Fig. 1B shows the C 1s spectrum. The five peaks at 284.6, 285.6, 286.9, 288.0, and 286.2 eV indicated the presence of C–C/C=C,[8] C–N,[18] C–OH,[19] N=C–N,[20] and C=O,[21] respectively. In the high-resolution N 1s spectrum, peaks at 398.6, 399.6, and 400.4 eV indicated the presence of C–N–C,[2] pyridinic N,[21] and C–$(N)_3$ (ref. 8, 22 and 23) (Fig. 1C). As illustrated in Fig. 1D, four peaks located at 531.6, 531.1, 533.0, and 535.5 eV confirmed the existence of C=O,[24] C–OH,[25] C–O–C,[26] and H–O–H,[25] respectively. Thus, the nitrogen-doped CDs are successfully synthesized using the electrochemical process.

The formation of the CDs was characterized using FT-IR (Fig. 2A). Peaks at 3000–3500 cm^{-1} confirmed the presence of OH/N–H bonds, and three peaks at 1617, 1566, and 1436 cm^{-1} confirmed the presence of C=O, C=C, and C–N bonds, respectively.[27] Moreover, C–N stretching of the amides peak was observed at 1376 cm^{-1}.[28] Fig. 2B presents a TEM image and reveals the size distribution of the CDs. The CDs were spheroidal and had an average diameter of approximately 5.17 nm.

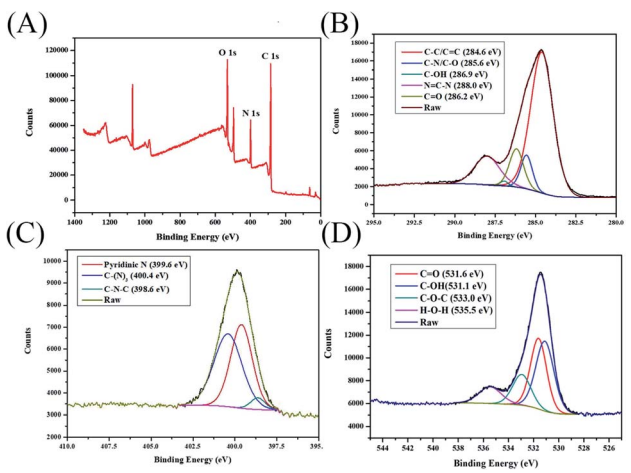

Fig. 1 (A) XPS survey spectrum CDs, and the corresponding high-resolution (B) C 1s, (C) N 1s, and (D) O 1s XPS spectra.

3.2 Optical properties of the CDs

UV/vis absorption and FL spectra were used to investigate the optical properties of the CDs. The UV/vis spectrum (Fig. 3A) exhibited two absorption peaks at 285 and 340 nm. The peak at 285 nm was induced by π–π^* transition of aromatic sp^2 domains from the carbon core. The peak discovered at 340 nm was attributed to n–π^* transition of the surface moieties with nitrogen atom.

The dispersion of CDs under 365 nm and 400 nm wavelength LEDs exhibited blue and green emission, respectively (Fig. 3A). The blue maximum emission at 440 nm was observed under maximum excitation wavelength at 325 nm, and the green maximum emission at 510 nm was observed under maximum excitation wavelength at 390 nm. Fig. 3B depicted CDs at 325, 390, 430, 470, and 500 nm excitation wavelength, respectively. The CDs exhibited different colors under various irradiation wavelength, which we believe ours to be suitable for biological imaging or application of optical components.

3.3 Stability of the CDs

Effect of ionic strength was investigated by treating the CDs with sodium chloride solutions of different concentrations (0.1–1 M). Fig. S1(A) and (B)† reveals that neither emission intensities changed considerably, even at high NaCl concentration. Thus, the CDs retain high fluorescent stability under high ionic strength condition and are suitable for the application of real environmental or biological samples. Effect of pH on CDs' emission spectra was observed through the addition of buffer solutions of different pH phosphates (pH 1–12). As depicted in Fig. S1(C) and (D),† the intensity of green and blue emission remained stable in solution of pH values in going from 2 to 12, which indicated that the obtained CDs are suitable for a wide range of applications.

Furthermore, the effect of organic solvents was also investigated through processing of the CDs with different solvents (Fig. S2†). Fig. S2(A)† reveals that the blue emission fluorescence intensity was considerably enhanced by addition of different solvents. However, the addition of organic solvents had no effect on the green emission fluorescence intensity (Fig. S2(B)†). We speculated that these two observations were attributable to different functional groups on the CDs, which caused different fluorescence properties in the organic solvent.

Subsequently, the fluorescence intensity signals of the CDs at different oxidizing/reducing agents were recorded. The results are displayed in Fig. S2(C) and (D).† The fluorescence intensity did not change for both emission wavelength of 440 nm and 510 nm. Next, the stability of the as-prepared CDs at 4 °C was investigated. As displayed in Fig. S3(A),† the CDs were stable for at least 1 months, making them beneficial for several applications. The zeta potential of the CDs is displayed in

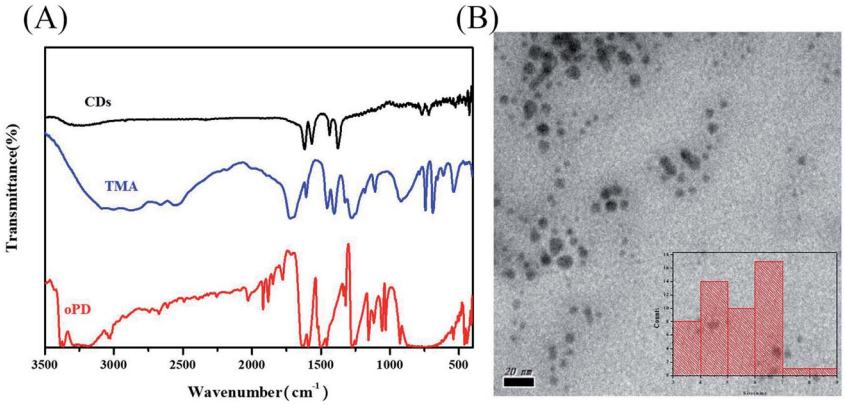

Fig. 2 (A) FT-IR spectra of trimesic acid, *o*-phenylenediamine and CDs. (B)TEM image of CDs. Inset: size distribution histogram based on counting 50 nanoparticles of CDs.

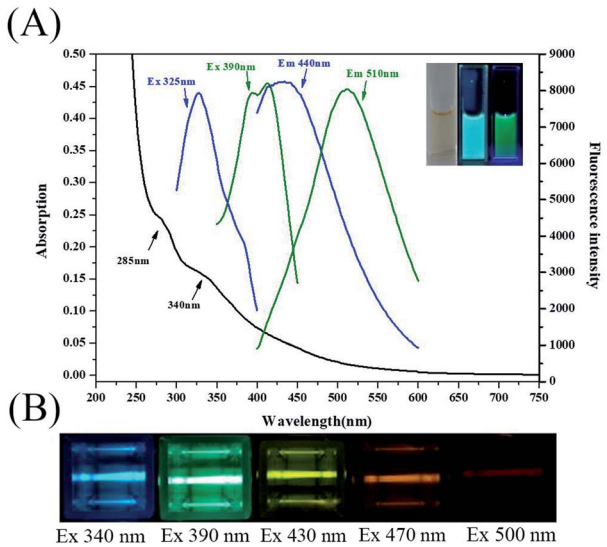

Fig. 3 (A) UV-vis absorption (black), excitation (pink and green) and fluorescence emission (red and blue) spectra of CDs. [Inset: photographs of CDs in visible-light (left) and under UV-light ex 365 nm(middle) and 400 nm(right)]. (B) Photographs of CDs under different excitation wavelength.

Fig. S3(B).† The surface zeta potential of the CDs was −30 mV, which is attributable to the presence of negatively charged acid and hydroxyl groups. Next, we investigated the resistance of our CDs to photobleaching through UV light illumination. As depicted in Fig. S3(C) and (D),† under continuous UV light (254 nm) illumination, the emission fluorescence intensity at 440 nm increased, whereas the emission fluorescence intensity at 510 nm did not changed. According to the report,[21] the photoexcited CDs are capable of producing reactive oxygen species (ROS). We conjectured that CDs generate ROS under UV light illumination.[27] The DCFH could be rapidly oxidized by ROS and lead to the formation of highly fluorescent 2′,7′-dichlorofluorescein (DCF) species.[29] The ROS generated from CDs under UV light irradiation could be verified by monitoring the DCF fluorescence signal (Fig. S4†). With continuous irradiation under a 365 nm UV lamp, the fluorescence intensity of DCHF/CD solution at 525 nm was considerably enhanced and higher than that under the condition without the CDs. Furthermore, we added acetylcysteine into the system as the ROS inhibitor. Fig. S4† reveals that acetylcysteine could successfully suppress the DCF fluorescence signal from the reaction between DCHF and ROS generated from the CDs under UV light. We believe that our CDs have potential to degenerate the organic pollution under UV light irradiation.

3.4 Determination of Hg^{2+}, glyphosate and HCQ

3.4.1 Sensitivity to Hg^{2+}. Fig. 5A reveals that the fluorescence of the CDs was considerably quenched by Hg^{2+} because of the interaction between the CDs and Hg^{2+}. Many functional groups, such as $-NH_2$ and –COOH, on the surface of CDs form complexes with Hg^{2+}.[30] The selectivity of other metal cations on the fluorescence detection of the CDs for Hg^{2+} was also investigated in this experiment. As depicted in Fig. 4, Hg^{2+} and Cu^{2+} induced a prominent fluorescence intensity reduction. A comparing the response of two emission fluorescence wavelengths to these metals revealed that the emissive wavelength at 510 nm was more sensitive than the emission wavelength of 440 nm. The selectivity of the CDs to Hg^{2+} suggested that the use of our CDs for sensing Hg^{2+} is feasible. With the continuous addition of Hg^{2+}, the fluorescence intensity of the CDs solution at 510 nm was considerably quenched and the fluorescence peak did not shift (Fig. 5A). A linear plot was obtained up to the Hg^{2+} concentration 50 μM, with a linear relationship $F/F_0 = 1.0081–0.01484$ (ref. 31) and R^2 of 0.9954. The limit of detection (LOD) for Hg^{2+}, according to the formula $3\sigma/S$, was 0.42 μM (Fig. 5B). The LOD of the proposed method for detecting Hg^{2+} was comparable to those of previously reported methods (Table S2†). To assess the applicability of the CDs, the tap water, lake water, and drinking water samples were conducted to estimate the possibility and reliability of the proposed method. The recovery percentage was calculated over a wide range of concentration (Table 1). The results indicated that the proposed method could be applied for the detection of Hg^{2+} ion in these water samples.

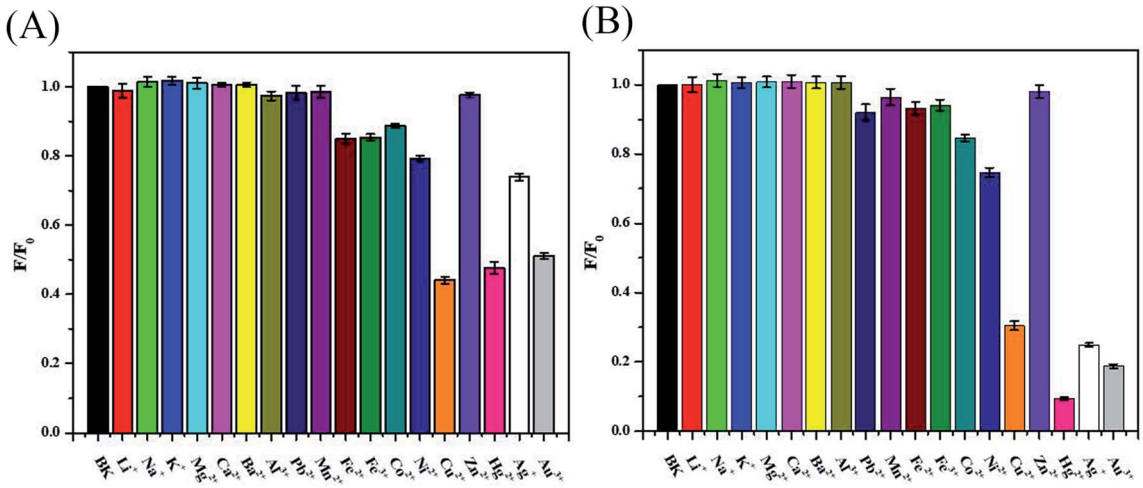

Fig. 4 Response of fluorescence intensity of CDs after the addition different metal ions (1 mM) at emission wavelength (A) 440 nm, and (B) 510 nm.

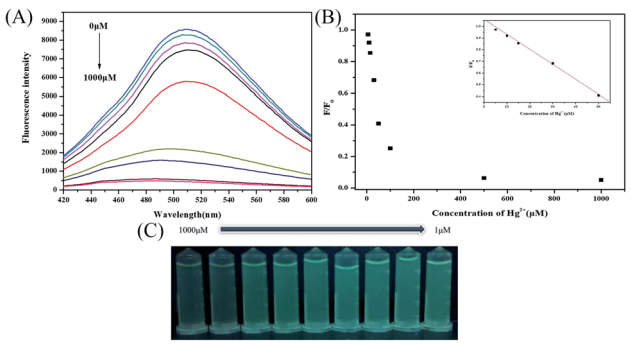

Fig. 5 (A) Change in fluorescence intensity of CDs on adding Hg^{2+}. (B) Linear plotting of F/F_0 *versus* concentration of Hg^{2+}. (C) Photographs of the corresponding detection condition.

Table 1 Analytical results for the detection of Hg^{2+} in different water samples

Sample	Spiked (μM)	Found (μM)	Recovery (%)	RSD (%) ($n = 3$)
Tap water	10	10.70	107.0	1.31
	25	28.02	112.1	1.20
	40	40.20	100.5	6.51
Drinking water	10	9.83	98.3	1.07
	25	26.30	105.2	1.65
	40	40.36	100.9	6.23
Lake water	10	11.01	110.1	2.00
	25	25.18	100.7	2.02
	40	41.00	102.5	1.10

3.4.2 Sensitivity to glyphosate. Fig. S5† reveals that an increase in the concentration of Cu^{2+} in solution efficiently quenched the fluorescence emission intensity of the CDs. Typically, glyphosate, which contains carboxyl groups and phosphonyl groups, can chelate with Cu^{2+}, which reduced the quenching effect of Cu^{2+} on CDs fluorescence.[32] After the addition of glyphosate into the CDs/Cu^{2+} system, considerable fluorescence recovery of the CDs was observed because of the competitive affinity to Cu^{2+} between glyphosate and the CDs (Fig. 6A).

To confirm that Cu^{2+} forms stable complexes with glyphosate, we also evaluated the zeta potential of the CDs/Cu^{2+} and the CDs/Cu^{2+}/glyphosate. As depicted in Fig. 6B, the zeta potential of the CDs dramatically changes from −30 mV to 4.26 mV after the addition of Cu^{2+}. After glyphosate was added to the CDs/Cu^{2+} system, the zeta potential changed from 4.26 mV to −27 mV, which proves the affinity between glyphosate and Cu^{2+}. Moreover, the selectivity of this proposed method for glyphosate detection was investigated. As depicted in Fig. 7, the fluorescence intensity did not changes obviously with the addition of other pesticides into the CDs/Cu^{2+} solution. The results reveals that our CDs/Cu^{2+} system exhibited a high selectivity for the detection of glyphosate. As illustrated in Fig. 8A, the fluorescence intensity of the CDs solution increased upon addition of glyphosate in various concentration (0–100 mg L^{-1}). A linear relationship in the concentration range of 2.5–25 mg L^{-1} of glyphosate is obtained. The equation of calibration curve and determination coefficient was $F/F_0 = 0.9688 + 0.0065$[glyphosate], and R^2 is 0.9954, where F and F_0 represented

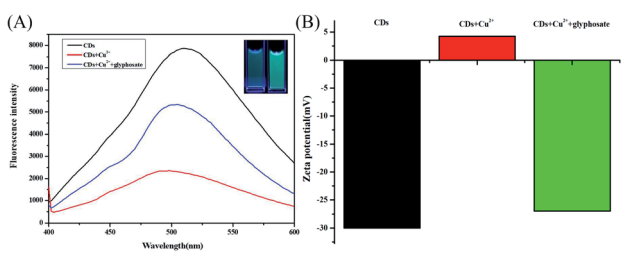

Fig. 6 (A) Fluorescence emission spectra of CDs, CDs/Cu^{2+}, and CDs/Cu^{2+}/glyphosate mixtures in an aqueous solution. [Inset: photographs of CDs/Cu^{2+} (left) and CDs/Cu^{2+}/glyphosate (right) under UV-light 400 nm]. (B) Zeta potential histogram of the CDs, CDs/Cu^{2+}.

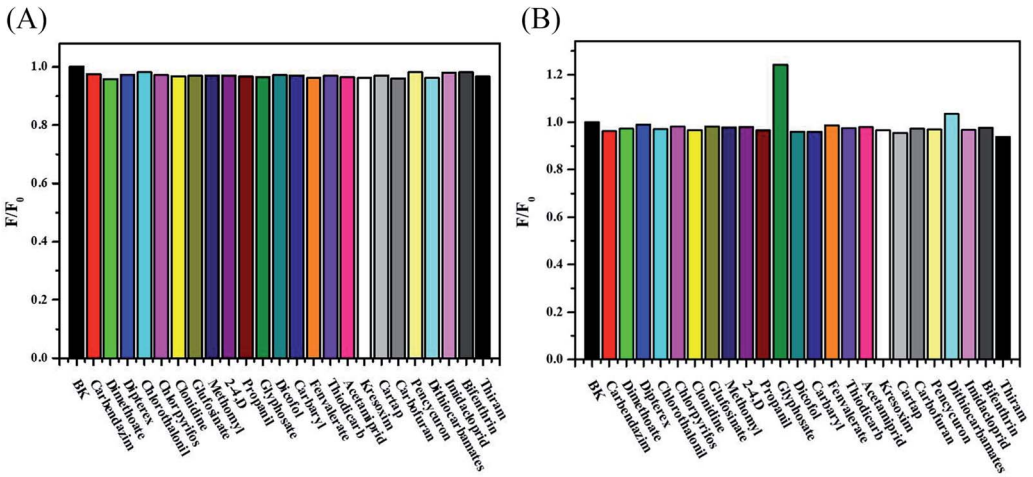

Fig. 7 (A) Response of fluorescence intensity of CDs after the addition different pesticides (100 ppm), (B) response of fluorescence intensity of the CDs/Cu^{2+} system towards pesticides.

Table 2 Analytical results for the detection of glyphosate in different water samples and cereals sample

Sample	Spiked (ppm)	Found (ppm)	Recovery (%)	RSD (%) ($n = 3$)
Tap water	10	11.56	115.6	3.11
Drinking water	10	10.61	106.1	1.70
Rice	10	9.83	98.3	0.85

the fluorescence intensity of the CDs/Cu^{2+} system in the existence and absence of glyphosate. The LOD ($3\sigma/S$) was 1.1 mg L^{-1}.

To demonstrate the analytical performance of this nanoprobe in water and cereals samples, the proposed method was applied to detect glyphosate in different sample matrixes. The results are listed in Table 2. The recoveries in the spiked water and cereals samples were in the range of 106.1% to 115.6% and the RSD is lower than 3.11%. The results reveals that the CDs/Cu^{2+} can be used as a reliable optical sensor for quantitative analysis of glyphosate (Table S3†). Although the detection limit in this work was not considerably better than that previously reported, it has a wide linear range and is simple. The result confirmed that this CDs/Cu^{2+} system can be used to detect the glyphosate in the water and cereals sample.

3.4.3 Sensitivity to HCQ. The as-prepared CDs with blue emission could be quenched when the HCQ was added to the CDs solution. The UV absorption spectrum of HCQ and the fluorescence spectrum of the as-prepared CDs are depicted in Fig. 9A. The UV-vis absorption spectrum of HCQ revealed two peaks at 325 nm and 330 nm, while the excitation wavelength of the CDs was at 325 nm. A possible fluorescence quenching mechanism of the CDs by HCQ is the IFE. After adding the HCQ into the CDs solution, the fluorescence intensity considerably decreased (Fig. 9B). The selectivity of the CDs was crucial for determination of HCQ in urine samples. The CDs fluorescence response with other correlative small molecules was investigated under the same conditions, as depicted in Fig. 10. In these spectra, no obviously changes in fluorescence intensity was observed when the aforementioned compounds were added in the aqueous dispersion of the CDs, which revealed that our CDs had the ability to recognize the HCQ. As illustrated in Fig. 11A, the fluorescence intensity of the CDs solution decreased with the addition of HCQ at different concentration (0–1000 μM). A

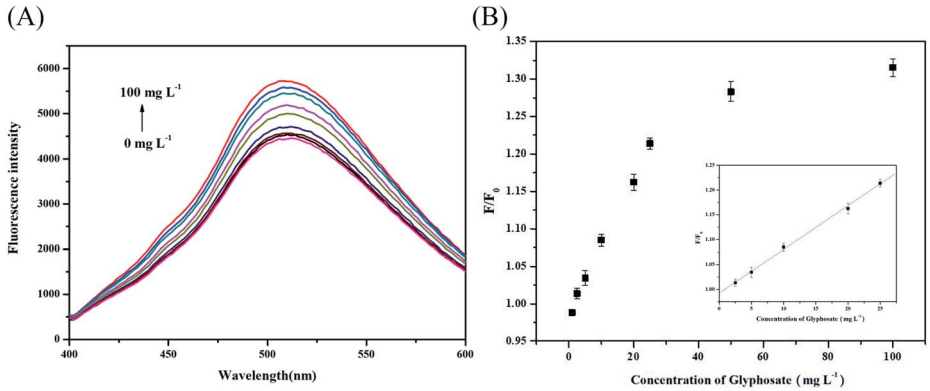

Fig. 8 (A) Change in fluorescence intensity of CDs on adding glyphosate. (B) Linear plotting of F/F_0 *versus* concentration of glyphosate.

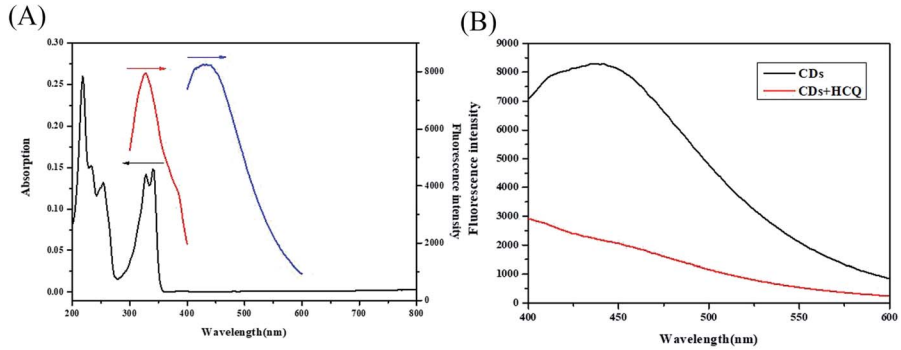

Fig. 9 (A) Fluorescence spectra spectrum of CDs under 325 nm exaction wavelength, and UV-vis absorption spectrum for hydroxychloroquine. (B) Fluorescence spectra of CDs before and after adding hydroxychloroquine.

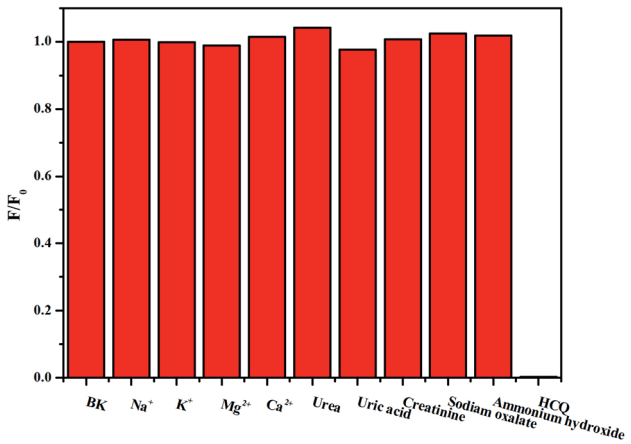

Fig. 10 Response of fluorescence intensity of CDs after the addition different metal ions and small molecules (1 mM).

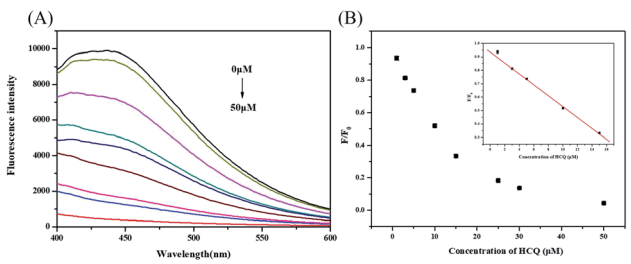

Fig. 11 (A) Change in fluorescence intensity of CDs on adding hydroxychloroquine. (B) Linear plotting of F/F_0 *versus* concentration of hydroxychloroquine.

linear plot was obtained for HCQ concentration up to 15 μM, with a linear relationship $F/F_0 = 0.093923–0.04063$[HCQ] and R^2 of 0.9971. The detection limit ($3\sigma/S$) was calculated to be 0.14 μM. The method was also applied to detect the HCQ in urine sample. The obtained urine samples were spiked with various concentration of HCQ and evaluate by using the proposed mechanism. Table 3 reveals that the recoveries were in the range of 97.2–114.7% for urine samples, with low relative standard deviation (<2.27%). These results indicated that the

Table 3 Analytical results for the detection of hydroxychloroquine in different urine samples

Sample	Spiked (μM)	Found (μM)	Recovery (%)	RSD (%) ($n = 3$)
Artificial urine	3	3.11	103.7	1.50
	5	5.74	114.7	1.48
	10	10.68	106.8	2.02
Human urine	3	3.09	103.0	1.08
	5	4.82	97.2	0.95
	10	10.76	107.6	2.27

CDs could be as promising fluorescent probes for assaying HCQ in urine samples. This fluorescence assay was applied successfully to the detection of the HCQ in urine samples and provided rapid screening and high throughput.

4. Conclusions

Duel-emission CDs were synthesized thought a one-step electrochemical synthesis under room temperature and pressure. Under these two excitations ($\lambda_{ex} = 325$ nm and $\lambda_{ex} = 390$ nm), the CDs exhibited two emission peaks at 440 nm and 510 nm. The as-prepared CDs were successfully applied for the detection of Hg^{2+}, glyphosate, and HCQ. The detection limit of Hg^{2+}, glyphosate, and HCQ were 0.42 μM, 1.1 mg L^{-1}, and 0.14 μM, respectively. Moreover, this assay was also applied to the different sample matrix such as water, cereals, and urine sample. This new designed CDs, with their special fluorescence property, are not only easy to prepare but also useful as multifunctional sensor for real samples.

Conflicts of interest

The authors have declared no conflict of interest.

Acknowledgements

This work was supported by the NTTU and Ministry of Science and Technology, Taiwan (MOST 109-2113-M-143-003).

References

1 C. Zhao, X. Li, C. Cheng and Y. Yang, *Microchem. J.*, 2019, **147**, 183–190.
2 J. Xia, S. Chen, G.-Y. Zou, Y.-L. Yu and J.-H. Wang, *Nanoscale*, 2018, **10**, 22484–22492.
3 X. Fu, R. Lv, J. Su, H. Li, B. Yang, W. Gu and X. Liu, *RSC Adv.*, 2018, **8**, 4766–4772.
4 Y. Fu, G. Gao and J. Zhi, *J. Mater. Chem. B*, 2019, **7**, 1494–1502.
5 Z. Ma, H. Ming, H. Huang, Y. Liu and Z. Kang, *New J. Chem.*, 2012, **36**, 861–864.
6 Y. Hu, Z. Yang, X. Lu, J. Guo, R. Cheng, L. Zhu, C.-F. Wang and S. Chen, *Nanoscale*, 2020, **12**, 5494–5500.
7 H. Yu, R. Shi, Y. Zhao, G. I. Waterhouse, L. Z. Wu, C. H. Tung and T. Zhang, *Adv. Mater.*, 2016, **28**, 9454–9477.
8 Y. Xu, D. Li, M. Liu, F. Niu, J. Liu and E. Wang, *Sci. Rep.*, 2017, **7**, 1–12.
9 B. Yuan, S. Guan, X. Sun, X. Li, H. Zeng, Z. Xie, P. Chen and S. Zhou, *ACS Appl. Mater. Interfaces*, 2018, **10**, 16005–16014.
10 Y. Liu, W. Duan, W. Song, J. Liu, C. Ren, J. Wu, D. Liu and H. Chen, *ACS Appl. Mater. Interfaces*, 2017, **9**, 12663–12672.
11 H. Zeng, L. Li, Y. Ding and Q. Zhuang, *Talanta*, 2018, **178**, 879–885.
12 S. Mohapatra, M. K. Bera and R. K. Das, *Sens. Actuators, B*, 2018, **263**, 459–468.
13 M. Harada, *Crit. Rev. Toxicol.*, 1995, **25**, 1–24.
14 Y.-C. Chang, Y.-S. Lin, G.-T. Xiao, T.-C. Chiu and C.-C. Hu, *Talanta*, 2016, **161**, 94–98.
15 D. Cressey, *Nature*, 2015, **24**, 1–3.
16 P. Colson, J.-M. Rolain, J.-C. Lagier, P. Brouqui and D. Raoult, *Int. J. Antimicrob. Agents*, 2020, 105932.
17 S. Zhang, Y. Bi, J. Li, Z. Wang, J. Yan, J. Song, H. Sheng, H. Guo and Y. Li, *Bioact. Mater.*, 2017, **2**, 53–62.
18 Y. Liang, Y. Shen, C. Liu and X. Ren, *J. Lumin.*, 2018, **197**, 285–290.
19 C. Fettkenhauer, X. Wang, K. Kailasam, M. Antonietti and D. Dontsova, *J. Mater. Chem. A*, 2015, **3**, 21227–21232.
20 F. Qiao, J. Wang, S. Ai and L. Li, *Sens. Actuators, B*, 2015, **216**, 418–427.
21 L. Shen, C. Wang, A. Abbas, C. Yu, S. Zhang, X. Zhang and C. Zhang, *ACS Appl. Nano Mater.*, 2019, **2**, 2776–2784.
22 L. Li, L. Shi, Y. Zhang, G. Zhang, C. Zhang, C. Dong, H.-Z. Yu and S. Shuang, *Talanta*, 2019, **196**, 109–116.
23 L. Shi, L. Li, X. Li, G. Zhang, Y. Zhang, C. Dong and S. Shuang, *Sens. Actuators, B*, 2017, **251**, 234–241.
24 X. Wang, Q. Chen, Z. Zhang, H. He, X. Ma, Z. Liu, B. Ge and F. Huang, *Colloids Surf., B*, 2019, **174**, 161–167.
25 R. Atchudan, T. N. J. I. Edison, K. R. Aseer, S. Perumal, N. Karthik and Y. R. Lee, *Biosens. Bioelectron.*, 2018, **99**, 303–311.
26 P. Das, S. Ganguly, M. Bose, S. Mondal, A. K. Das, S. Banerjee and N. C. Das, *Mater. Sci. Eng., C*, 2017, **75**, 1456–1464.
27 J. Xia, X. Wang, S. Zhu, L. Liu and L. Li, *ACS Appl. Mater. Interfaces*, 2019, **11**, 7369–7378.
28 Q. Ye, F. Yan, D. Shi, T. Zheng, Y. Wang, X. Zhou and L. Chen, *J. Photochem. Photobiol., B*, 2016, **162**, 1–13.
29 Y. Koide, Y. Urano, S. Kenmoku, H. Kojima and T. Nagano, *J. Am. Chem. Soc.*, 2007, **129**, 10324–10325.
30 A. Iqbal, K. Iqbal, L. Xu, B. Li, D. Gong, X. Liu, Y. Guo, W. Liu, W. Qin and H. Guo, *Sens. Actuators, B*, 2018, **255**, 1130–1138.
31 X. Zhang and Y.-Y. Zhu, *Sens. Actuators, B*, 2014, **202**, 609–614.
32 L. Wang, Y. Bi, J. Gao, Y. Li, H. Ding and L. Ding, *RSC Adv.*, 2016, **6**, 85820–85828.